Zone-center instability of C(5,0) carbon nanotubes inside $AlPO_4$-5 channels

M. V. Fernández-Serra[1,2] and X. Blase[3,4]
[1]*Department of Physics and Astronomy and New York Center for Computational Science, Stony Brook University, Stony Brook, New York 11794-3800, USA*
[2]*CECAM-ENS Lyon, 46 allee d'Italie, 69007 Lyon, France*
[3]*Institut Néel, CNRS and Université Joseph Fourier, BP 166, 38042 Grenoble Cedex 9, France*
[4]*Laboratoire de Physique de la Matière Condensée et Nanostructures (LPMCN), UMR CNRS 5586, Université Claude Bernard Lyon 1, Bâtiment Brillouin, 43 Bd 11 Novembre 1918, 69622 Villeurbanne, France*
(Received 25 February 2008; revised manuscript received 21 April 2008; published 15 May 2008)

The electronic structure of C(5,0) carbon nanotubes inside zeolite channels is analyzed. We confirm the occurrence of the metal-semiconductor transition which has been previously predicted in the case of isolated tubes. The interaction with the zeolite matrix does not prevent the spontaneous metal-semiconductor instability at room temperature, even though it reduces the magnitude of the band gap in the distorted stable phase. An empirical potential modeling, which allows the study of the tube and zeolite relaxation without the constraint of periodic boundary conditions, does not lead to the conclusion that some tubes could remain metallic.

DOI: 10.1103/PhysRevB.77.195115 PACS number(s): 73.22.−f, 74.10.+v, 71.20.−b, 71.15.−m

I. INTRODUCTION

The discovery of superconductivity (SC) correlations in single wall carbon nanotubes (SWCNTs), either in bundle geometries[1,2] or embedded in a zeolite matrix,[3] has inspired recent theoretical[4–8] and computational modeling[9–12] research on these systems, motivated by the challenge of understanding the origin of the SC transition in strictly one dimensional (1D) structures; see Ref. 13 for a review. Several pieces of evidence point to small diameter carbon nanotubes (CNTs) as being at the heart of the strongest observed SC correlations, leading to the highest observed T_c.[3] Firstly, the channels in the zeolite crystals of Ref. 3 only allow the growth of 4 Å diameter tubes. Additionally, it is well known that both the density of states at the Fermi level and the electron-phonon interaction are strengthened due to the increased curvature in these small tubes.[9,14,15] Finally, a recent experimental work has found a new SC transition in multiwall CNTs (MWCNTs) grown inside large zeolite channels with T_c up to 12 K.[16] This high T_c, very close to the one observed in the experiments by Tang *et al.*,[3] together with some evidence inferred from the experiments[17] in Ref. 16 point to the smaller tubes inside the MWCNTs as being responsible for the SC transition. If this is the case, it is quite possible that the SC found in these two very different experiments could be driven by the same physical mechanism. However, SC in small radius CNTs competes with other instabilities arising in the low energy excitation phase diagram of 1D systems. The aforementioned strengthening of the electron-phonon interaction in these systems also favors the occurrence of a charge density wave transition, manifested through a modulation of the charge density with a wave vector $q=2k_F$, k_F being the Fermi wave vector. Also known as a Peierls transition,[9,15,18] we will refer to it in more general terms as a metal-semiconductor transition (MST).

This MST has been shown to happen at room temperature in isolated C(3,3) tubes,[9,10] mediated by an optical phonon at $q=2k_F$. Due to curvature effects, $2\pi/2k_F$ in this tube is not commensurate with the unit cell vector along the axis direction, and therefore very large supercells are necessary to directly study the band-gap induced by the MST.[19] By contrast, the so called pseudo-Peierls[15] transition observed in the C(5,0) tube is the result of an spontaneous zone-center deformation, opening a gap of ≈0.2 eV, as obtained by Connétable *et al.*[9] in a study performed for isolated tubes.

While isolated C(5,0) and C(3,3) tubes have been extensively studied within density functional theory and Luttinger liquid framework,[6–8] only one study[20] has reported *ab initio* calculations of small radius CNTs including the zeolite channel. Further, the growth of defective tubes, accounting for tube-zeolite interactions, has recently been modeled by means of Monte Carlo simulations.[21] A detailed study of the effects induced by the zeolite network on the electronic properties of SWCNTs grown inside their channels is clearly needed in order to shed more light on the origin of the observed superconducting transition.

In this paper, we analyze in detail the electronic structure of the C(5,0) tube inside $AlPO_4$-5 (AFI) zeolite crystals by means of *ab initio* simulations. We show that the zone-center deformation observed in "isolated" tubes[9] does not disappear when the AFI matrix is also included in the calculations. Despite its insulating character, the AFI structure around the tube plays an active role, manifested in the reduction of the C(5,0) band-gap opened after the deformation of the tube. A structural coupling between the tube and the AFI channels is observed. We address the question of whether this coupling could, in principle, prevent the onset of the spontaneous deformation resulting in the MST, by modeling the interaction of the tube and the zeolite with a very simple force-field model that accounts for the zeolite flexibility. Our results indicate that the band-gap opening, while reduced, remains.

The paper is structured as follows: In Secs. II and III, we present the technical details of our calculations, including an analysis of the band structure of the isolated tubes, extending the results previously published by one of us[9] on the characterization of the MST. In Sec. IV, we study the zeolite-CNT complex. Section V presents the results for a simple classical model that addresses the question of the effect of the

TABLE I. Energies and geometries of the relaxation of the C(5,0) tube as a function of the size of the cell (hexagonal unit cell) characterized by the intertube distance [D (T-T)] and as a function of the calculation method (LCAO stands for linear combination of atomic orbitals and PW for plane waves). $E_{sph}-E$ is the difference in total energy between the fully relaxed nondeformed structure and the fully relaxed deformed one. ΔE^1_{gap} is the energy band gap at Γ and ΔE^2_{gap} is the band gap along the intertube dispersion direction. $R1/R2$ is the ratio between the two in equivalent radii of the deformed tube.

Method	Initial structure	D (T-T) (Å)	$E_{sph}-E$ (eV)	ΔE^1_{gap} (eV)	ΔE^2_{gap} (eV)	$R1/R2$
LCAO	Sphe	21.0	0.0	0.0	0.0	1.0
LCAO	Def[a]	21.0	0.017	0.15	0.15	0.97
LCAO	Def[a]	11.0	0.020	0.17	0.17	0.97
LCAO	Def[a]	4.0	0.382	0.25	0.02	0.97
PW	Sphe	9.6	0.0	0.0	0.0	1.0
PW	Def[a]	9.6	0.01	0.17	0.17	0.97
PW	Sphe	5.0	0.2	0.35	0.05	0.97

[a]The starting deformed structure corresponds to the fully relaxed structure obtained after the simulation in the last line of the table.

periodic boundary conditions imposed by our *ab initio* simulations. Conclusions are presented in Sec. VI.

II. METHODOLOGY

We have performed *ab initio* simulations both with the use of plane waves[22] and strictly localized numerical atomic orbitals[23] (NAOs). Plane wave calculations were performed on "isolated tubes" in order to compare and validate the localized orbitals approach that is used throughout the study.

A. Plane waves

Total energy and stability studies of the tube have been performed both with the use of norm conserving[24] and ultrasoft pseudopotentials.[25] The electronic eigenstates were expanded on a plane wave (PW) basis of 50 Ry cutoff that was reduced to 30 Ry when ultrasoft pseudopotentials were employed. We used a hexagonal cell with two different vacuum distances between the tubes, 4 and 15 Å, in order to analyze the effect of bundling geometries. The lattice parameter along the axis direction was optimized until the vertical stress was less than 10 kbar. We have performed calculations both within the local density approximation (LDA)[26,27] and the generalized gradients approximation (GGA)[28] to the exchange correlation potential. A minimum of 50 k points were used to sample the Brillouin zone along the nanotube axis direction, ensuring the k-point convergence required for this type of systems.[18] In all the calculations, the total energy is calculated taking into account an electronic entropic correction due to the Fermi-Dirac distribution to populate the energy levels. This method explicitly accounts for the effect of the temperature, which is set to 300 K, within the so-called Mermin generalization of density functional theory (DFT) to finite temperatures.[29]

B. Numerical atomic orbitals

The studies for the isolated tubes and also for the complex $C(5,0)+AlPO_4$-5 have been performed in parallel within a localized-basis implementation of DFT. The eigenstates of the Kohn-Sham Hamiltonian are expressed as linear combinations of NAOs.[23] These NAOs are strictly localized, i.e., their radial functional form is zero beyond a given cutoff radius. We have used a double-ζ polarized basis, with orbital radii up to 6.8 a.u., variationally optimized to better describe C atoms in graphenelike environments.[30,31] Real space integrals were performed on a mesh with a 310 Ry cutoff.[23] The unit cell c axis was optimized to obtain stress values similar to the ones computed in the PW simulations. Atoms in the zeolite were also described using a double-ζ polarized basis set with orbital radii up to 8 a.u. for Al, 6.2 a.u. for O, and 6 a.u. for P. We have tested that our results do not depend on the quality of the basis used to describe the zeolite matrix, as long as it is good enough to properly describe the interactions between the two systems.

III. C(5,0) TUBES ISOLATED

The two methods have been compared in the case of isolated tubes and shown to produce identical results. By isolated tubes we mean here that a distance of about 15 Å between tube walls was imposed within our periodic boundary conditions approaches. The description of the tube has been carefully tested for different convergence parameters and different approximations, in order to eliminate the possibility of spurious errors at the origin of the spontaneous deformation of the tube.

A. Electronic band structure

Results for the different calculations are presented in Table I. In particular, we have seen that none of the approximations involved in the DFT method (LDA versus GGA, the use of different pseudopotentials, quality of the basis) compromise the main result of the simulations, i.e., the observation of a zone-center deformation of the tube, opening a gap of $\approx$0.2 eV.

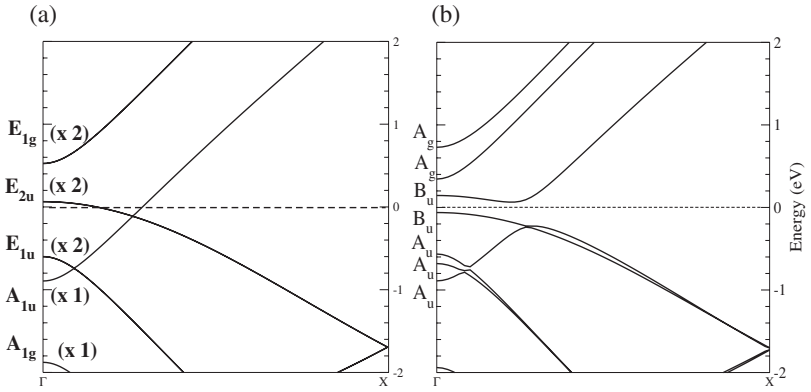

FIG. 1. Band structure of the (a) undeformed and (b) deformed tubes. The Fermi level is set to zero in both graphs and indicated with a discontinuous line. The labels for the symmetry representations of the relevant bands around the Fermi level are indicated; in (a) the numbers on the dispersion curves indicate their degeneracy. (a) D_{5d} and (b) C_{2h} point groups.

However, this deformation is spontaneous only if the size of the unit cell allows for lateral dispersion. In other words, a bundlelike arrangement of the tubes will induce a symmetry breaking which will drive the system into an insulating state. While such a bundle geometry does not reflect the actual geometry of zeolite-inserted tubes, it is instructing to discuss here the effect of breaking the D_{5d} symmetry by lateral interaction in the hexagonal periodic packing geometry.

We have studied the band structure of the nanotube around the Fermi level as a function of the intertube distance. The band structure of the D_{5d} symmetric tube is shown in Fig. 1(a). While the graphene band folding scheme for this tube results in a semiconducting structure, the small curvature of the tube induces a π-σ rehybridization of the C orbitals and, as a consequence, the system shows a strong metallic character.[32] The Fermi level intersects two different bands, one of which (label E_{2u}) is doubly degenerate.

As can be seen in the table, when the intertube distance is large enough to prevent the symmetry breaking, the tube will remain metallic after relaxation (starting from the totally symmetric D_{5d} configuration). Nonetheless, the most stable state will be still the semiconducting tube, although the difference in energy is very small, of $\approx$0.02 eV. Therefore, the picture that emerges from these calculations, as sketched in Fig. 2, is the following: the potential energy surface (PES) of isolated tubes presents a double well potential with a nonglobal metallic minimum and a semiconducting global minimum. We have calculated the phonon modes by means of finite differences for the metallic isolated tubes. The absence of negative modes confirms the existence of two real minima. In a bundlelike geometry, the PES of the tube changes; as soon as the symmetry is broken through the tube-tube interaction (in the hexagonal periodic configuration we adopted), a splitting of the double degenerated E_{2u} band is observed, spontaneously driving the system into the semiconducting structure which becomes the only minimum. The potential profile leading from the symmetric to the distorted structure is found to be very flat (see Fig. 2); if the transition is to be observed by means of standard geometry optimization methods, a very low tolerance in the forces will be required. Otherwise, the instability of the metallic state can be shown by the negative mode appearing in the phonon calculation. This spontaneous deformation of the tube has been originally labeled as a pseudo-Peierls transition.[9,15] However, the name is misleading, given that it occurs at Γ. As can be appreciated from Table I, the deformation energy gain ($E_{spheric}-E_{distorted}$) increases with decreasing intertube distance [D(T-T)]. As for the electronic properties, the closer the tubes, the larger the band gap opening at Γ. Nonetheless, as soon as tubes come close to each other (here for distance smaller than 4.0 Å), tube-tube lateral interactions start inducing a dispersion of the bands in the transverse direction. Such an evolution and its consequences can be clearly seen in Fig. 3 with a reduction of the band gap along the MK direction of the hexagonal Brillouin zone. This closing of the band gap in nanotube bundles has already been shown to occur by Reich *et al.*[33] We will come back to this band-gap reduction by lateral interaction in the case of zeolite-intercalated tubes.

B. Symmetry analysis

The tube undergoes a symmetry transformation from the D_{5d} group toward the C_{2h} group.[34] Figure 4 shows the wave functions at Γ for the doubly degenerate state involved in the transformation (E_{2u} state). The *ungerade* symmetry of the state is evident in the plot. We have assigned the symmetry labels to the states looking at the wave functions at Γ. Our assignments differ from those previously given by Li *et al.*[35,36] We believe that a correct understanding of the symmetry of the states can help in the identification of dipole transitions contributing to the optical absorption spectrum.

The doubly degenerated E_{2u} states become B_u states after the symmetry transformation. Several authors[20,35,37] have

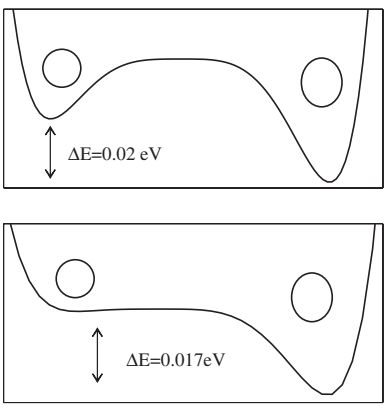

FIG. 2. Sketch of the potential energy surface of the C(5,0) tube as a function of the axial deformation. (a) Isolated tubes, double well potential surface type, with a global minimum at the deformed tube structure. (b) Bundle of tubes, the tube-tube interaction induces a breaking of the D_{5d} symmetry and only one minimum exist.

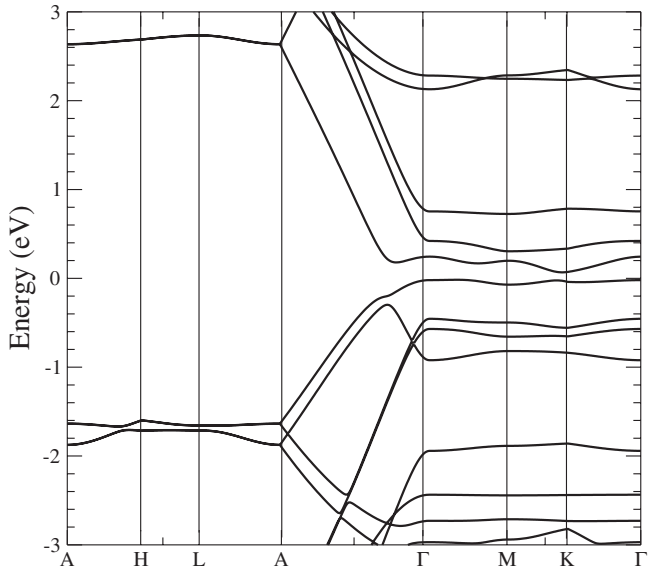

FIG. 3. Band structure of a bundle of C(5,0) nanotubes with 4.0 Å interwall distance. While the direct energy band gap at Γ is ≈0.2 eV, there is a tendency to close the gap at the K point of the hexagonal Brillouin zone (E_{gap}=0.08 eV).

calculated the optical absorption spectrum by computing the imaginary part of the dielectric function using first order time-dependent perturbation theory to calculate the dipolar transition matrix elements between occupied and empty single electron eigenstates. The $D_{5d} \rightarrow C_{2h}$ symmetry transformation would also have an effect in the calculated absorption spectrum. The splitting of the states would change the spectral features associated with the $E_{1u} \rightarrow E_{1g}$ dipole transition. This transition was identified[35,37] as the one contributing to the characteristic C(5,0) signal in the absorption spectrum, at around 1.37 eV.[35] Obviously, in the deformed tube, there would be two allowed dipole transitions, corresponding to the split levels ($A_u \rightarrow A_g$), as can be seen from the band structure in Fig. 1(b). This could explain the observed shoulder in the optical adsorption spectrum[35] around 1.2 eV, which could be related to the splitting presented here becoming an experimental evidence of the occurrence of the tube deformation at room temperature.

IV. C(5,0)+AlPO$_4$-5 MATRIX

Having seen that the symmetry breaking of the tube is a consequence of the tube-tube interaction, it is clear that the analysis of the electronic structure should be performed accounting for the experimental conditions, i.e., taking into account the effects of the zeolite matrix on the stability and electronic properties of the tube. It is only after considering the band structure of the tube inside the zeolite that we will be able to compare theoretical results to experimental data, given that experiments are always performed for the tubes inside the zeolite channels.

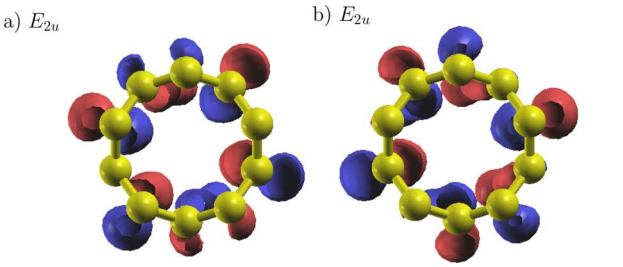

FIG. 4. (Color online) Transversal cross section of the wave functions 40 and 41 at Γ before (E_{2u}) the deformation of the tube and opening of the gap. The ungerade character of the states is evident in the plot.

A. 1×1×2 unit cell

Figure 5(a) shows a view of the unit cell of the AFI crystal with the symmetric C(5,0) tube inside, along the [001] direction. The c axis of the AFI unit cell is almost commensurate with two unit cells of the nanotube as shown in Fig. 5(b).

The complex (tube+zeolite) unit cell comprises a total of 114 atoms (74 from the matrix and 40 from the tube). Total energy calculations and relaxations of the structure have been performed with the SIESTA method. We have imposed the periodicity of the system along the c axis according to the optimized c lattice parameter of the C(5,0) tube found in the previous section. The unit cell parameters used in the AFI+C(5,0) complex calculations were a=13.8 Å and c=8.5 Å; this can be compared to the experimental c-axis value of 8.4 Å as reported by Launois *et al.*[38,39] We have conducted a number of structural relaxations imposing different constraints on the atoms in the system. Initially, only the C(5,0) tube was allowed to relax, but conservation of the D_{5d} symmetry was imposed. The two E_{2u} states therefore remain degenerate, and no important changes in the band structure as compared to that of the isolated tube are observed. This implies that the zeolite matrix plays no relevant role on screening the intratube Coulomb interactions. With a doubling of the nanotube unit cell, the tube band structure is folded onto half of the irreducible tube Brillouin zone. Due to the large zeolite band gap (6 eV), the tube-originated

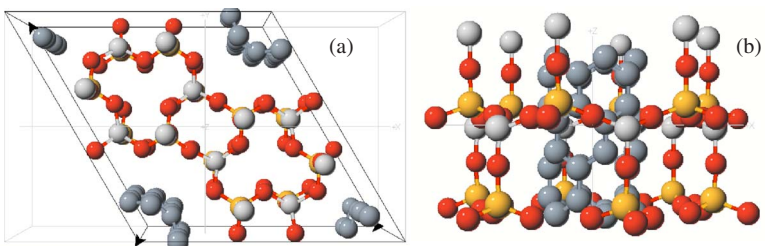

FIG. 5. (Color online) (a) Unit cell of the C(5,0)+AlPO$_4$-5 complex seen along the [001] direction. (b) Lateral view of the unit cell showing the very good match between O rings and C(5,0) carbon zigzag chains.

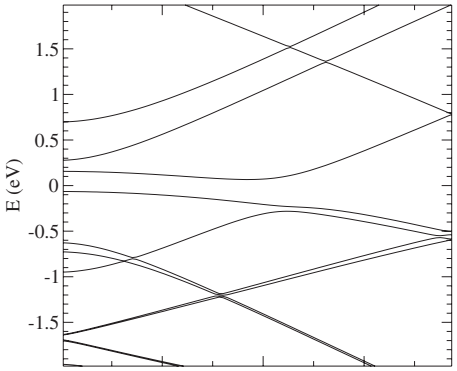

FIG. 6. Band structure around the Fermi level for the distorted tube inside the zeolite channel.

bands are easily identifiable around the Fermi level. The position of the Fermi level with respect to the tube bands as compared with the isolated tube does not change, an indication of the absence of charge transfer between the two systems and therefore of no relevant tube-zeolite interaction. If the symmetry constraint on the tube is released, but the zeolite frame is kept rigid, the splitting of the bands occurs, but the tube never undergoes the expected MST, even imposing a tolerance in the forces of 0.005 eV/Å, much smaller that the one used to see the transition on the isolated tubes. Once all the constraints are released, the interactions between the tube and the zeolite are allowed to switch on, and both structures relax together. As a result, the tube undergoes the same zone-center distortion as observed in the isolated structure. The electronic band structure around the Fermi level is shown in Fig. 6.

The band gap is reduced by ≈20%, as a result of the interaction between the AFI matrix and the tube. The AFI channels also distort, as can be noticed in Figs. 7(a) and 7(b). Floppy modes of the zeolite framework associated with rotations of the AlO_4 and PO_4 tetrahedra and induced by interactions between C atoms in the tube close to O rings in the zeolite deform the AFI matrix with a very low energy cost. Since allowing the zeolite to relax favors the tube deformation (see above), one concludes that the energy cost associated with changing the zeolite tetrahedra orientation is smaller than the interaction energy between the tube and the zeolite. While it is commonly assumed that the zeolite plays the role of an inert host matrix, our results show that the tube-matrix interaction is of great significance, at least at the scale of the energies involved in the tube deformation. In particular, and that is the main result of the present study, the zeolite does not quench the tube deformation but on the contrary favors it. We can estimate the strength of the C-O interaction by looking at the "binding" energy between the two systems E_{int}, defined as $E_{int}=E_{complex}-E_{AFI}-E_{tube}-E_{BSSE}$, where BSSE stands for basis set superposition error.[40] We have calculated this interaction for the fully relaxed structure which comes out to be of about 0.5 eV per unit cell, that is, around 13 meV/atom.

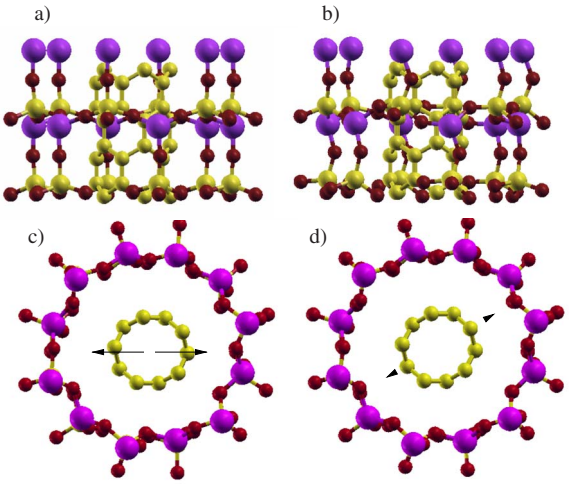

FIG. 7. (Color online) (a) Side view of the undistorted AFI-C(5,0) complex. (b) Side view of the complex after distortion of both the AFI channels and C(5,0) CNT. (c) Top view of a distorted CNT inside the AFI channel with its distortion axis indicated. (d) The distortion axis changes after the tube is rotated and let to relax again.

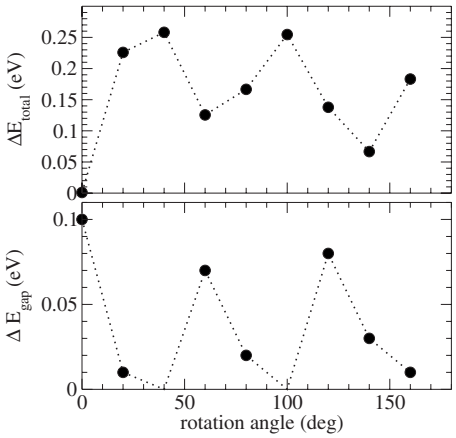

FIG. 8. Evolution of the total energy (top) and band-gap energy for a distorted tube as a function of its rotational angle around its own axis.

However, not all C atoms interact equally with their nearest O atoms. Indeed, in the structure, only a number of carbon atoms are at an optimum distance from their nearest O neighbors. Because of this, the deformation axis [see Figs. 7(c) and 7(d)], which should, in principle, be fivefold degenerate, is determined by the rotational angle of the tube inside the channel. Indeed, the potential energy as a function of this rotational angle is periodic, with period of $\pi/6$, corresponding to the sixfold axis of the oxygen rings in the AFI channels. This can be observed in Fig. 8, where we plot the total energy of a semiconducting C(5,0) tube as a function of its rotational angle inside the zeolite channel (note the we do not relax the structure after each rotation).

In the same figure, we also show how the band gap is affected by this periodic potential. In addition, the dependence of the deformation axis on the rotational degree of freedom of the tube is supported by the result shown in Fig. 7. A fully relaxed tube (therefore semiconducting) is rotated 40° inside the AFI channel and the structure is allowed to relax again. As can be seen in the figure, the deformation axis changes, the new one being determined by those carbon atoms closer to oxygens in the ring.

B. 1×2×2 unit cell

The previous study reveals that the band gap of the CNT after the MST is strongly dependent on its orientation inside the zeolite and on the response of the zeolite frame to the tube distortion. We have seen that this response depends on the orientation of the tube inside the channel, and therefore the question of whether tubes in neighboring channels with different orientations could induce competing deformations of the zeolite that might prevent or harden the MST still remains.

We explore this possibility in this section by considering a two unit cell system, with two channels and two tubes inside. After doubling the unit cell, we rotate $\pi/4$ one of the tubes around the C axis to ensure two different orientations and let the system relax. The initial structure of both tubes is taken after the MST; they are therefore distorted but have two different distortion axis. As expected from Fig. 7, the rotation of one of the tubes already reduces its band gap by ≈25% even without optimizing the geometry of the system. After fully relaxing the system, the band-gap reduction increases up to 40%, being of the order of 80 meV. Therefore, even if the semiconducting character of the tubes persists, it is clear that the interactions with the zeolite frame could drastically reduce the average band gap of the system.

V. CLASSICAL FORCE FIELD MODEL: MULTIPLE CHANNELS

The AFI matrix contributes to reduce the band gap as a result of a balance between different interactions. On one side, it is energetically favorable for the tubes to undergo a MST. Some C and O atoms establish an attractive interaction that "pulls" the walls of the AFT channel to follow the tube deformation, but the zeolite deformation is limited by its own rigidity. Different orientation of the tubes will induce different deformation forces in the channels's walls that at the end will limit the final deformation of the tubes. In order to see the effect of periodic boundary conditions with multiple channels, we have modeled this effect by designing a classical force field which takes into account all these effects. We simulate how the zeolite frame can respond to different orientations and deformations of the tubes by keeping fixed the C positions and letting relax the AFI structure. Our aim is not to obtain accurate energies but to study the effects on the rigidity of the AFI matrix as we increase the number of channels and tubes in the system.

A. Model force field

The zeolite force field aims to describe in the most simple way the elasticity of the frame, under deformation forces induced by the tubes inside the channels. It should properly characterize rigid rotations of the AlO_4 and PO_4 tetrahedra and bending and stretching motions of first nearest neighbor bonds. We use a straightforward harmonic bond model:[41]

$$U = \sum_{ij} K_{ij}^{s}(r_{ij} - r_{ij}^{0})^2 + \sum_{ijk} K_{ijk}^{b}(\theta_{ijk} - \theta ijk^{0})^2, \qquad (1)$$

where K_{ij}^{s} and K_{ijk}^{b} stand for the stretching and bending constants of the bonds. The parameters should be realistic and correctly reproduce the ratio between the different constants. In Table II, we present the parameters we used in our model, following the experimental results for the relevant vibrational modes presented in Refs. 42 and 43. Bond bending constants are assumed to be ten times smaller than the bending constants of the two (identical) bonds they join. Only bending motions inside the tetrahedra (P-O-P and Al-O-Al) are considered. The tube-zeolite interactions are modeled by a simple Lennard-Jones force field, between the carbon atoms and the oxygen rings that form the channel. The depth of the Lennard-Jones well, σ, is a variable parameter that determines the strength of the C-O interaction and that we assume to be between 10^{-2} and 10^{-3} times the energy of the covalent bonds in the zeolite structure. The minima of the well are fixed at the original distance between C and O atoms in the undistorted (but relaxed) structure, as obtained in our *ab initio* simulations. We build supercells with different numbers of unit cells in the XY plane ($n \times m \times 2$), where inside each of the channels we introduce a distorted C(5,0), with a randomly imposed distortion axis. The tubes are constrained and we let the zeolite geometry relax by minimizing the total energy using a conjugated gradients minimization method.

TABLE II. First line, force constants for the stretching (K^s, in eV/Å^2) and bending (K^b, in eV/Rad^2) of the zeolite bonds used in the model force field. Also in this line, depth of the Lennard-Jones potential (ϵ) used to describe the C-O interaction. Second line, equilibrium bond distances in the zeolite and σ constant for the C-O Lennard-Jones potential, all in Å.

$K_s^{\text{O-P}}$	$K_s^{\text{O-Al}}$	$K_b^{\text{Al-O-Al}}$	$K_b^{\text{P-O-P}}$	$\epsilon_{\text{O-C}}$
1.9	18.0	1.8	0.19	10^{-3}–10^{-4}
$r_0^{\text{(O-P)}}$	$r_0^{\text{(O-Al)}}$	$\theta_0^{\text{(Al-O-Al)}}$	$\theta_0^{\text{(P-O-P)}}$	σ
1.524	1.727	109.5°	109.5°	2.474

B. Model results and discussion

This simple model captures all the relevant physical interactions necessary to evaluate the response of the zeolite under different stresses in different channels. Indeed, we see a very similar relaxation of the zeolite as compared to the one we observe by means of *ab initio* calculations. The P-O-Al bridges along the c-axis direction, originally linear, bend forming angles of $\approx \pm 153°$. While the average angle for the whole structure is still 180°, there is an evident phase transition, which has been thoroughly analyzed by Bordat *et al.* showing that the structure with linear oxygen bridges corresponds to a saddle point of the potential energy surface. The growth of tubes inside the channels triggers the phase transition by breaking the original hexagonal symmetry of the structure.

We show in Fig. 9 the elastic energy cost per unit cell (or channel) as a function of the number of channels in the system and for different values of ϵ, the depth of the Lennard-Jones interaction potential between C and O atoms. We vary ϵ between 10^{-3} and 10^{-2} times the value of the stronger AFI

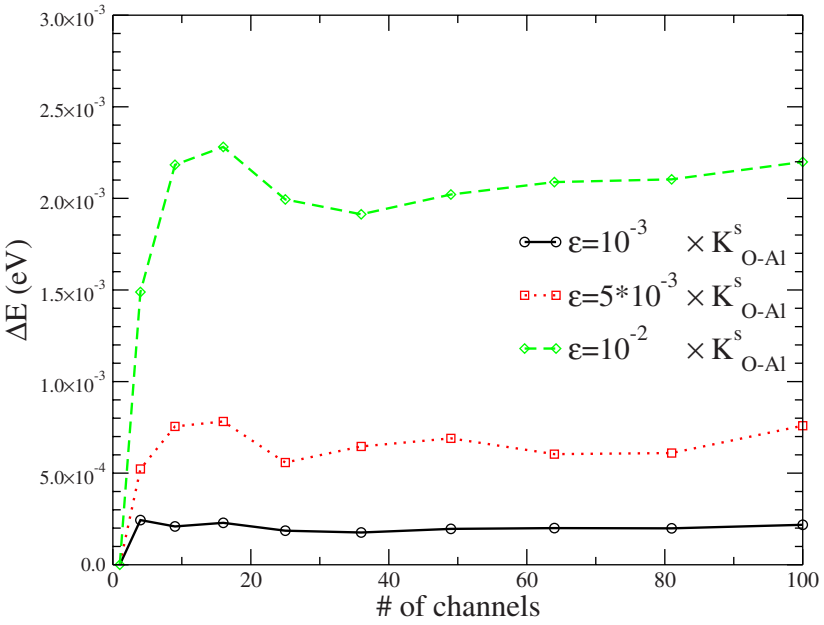

FIG. 9. (Color online) Elastic energy stored in the zeolite frame per channel as a function of the total number of channels and tubes (see text).

interatomic force constant $K^s_{\text{O-Al}}$ (see Table II). The elastic energy is calculated as the difference between the zeolite total energy at the relaxed structure (with a distorted tube inside the channel) for only one unit cell and the same energy per unit cell, for a variable number of channels with distorted tubes inside and randomly rotated. It can be seen that there is always a very small energy cost due to the fact that the rigid units in the zeolite cannot freely rotate without energy cost when tubes in neighboring cells induce competing deformations. However, this cost is negligible compared to the carbon nanotube band gap ($\approx 2 \times 10^{-3}$ eV for the largest interaction constant).

VI. CONCLUSIONS

The present study has been undertaken to understand the metal-semiconductor transition predicted to occur in isolated C(5,0) CNTs at room temperature. In particular, we have evaluated the effect of periodic boundary conditions on such a transition, showing that no matter which is the intertube distance, the absolute minimum of the potential energy corresponds to the distorted and semiconductor structure. We have also considered explicitly the role of the $AlPO_4$-5 zeolite matrix in the relaxation of the CNT structure. Our results indicate that while the interaction between the zeolite structure and the C(5,0) tube is larger than expected, the opening of the band gap still occurs. However, the band gap is reduced, our estimate being by more than 50%. This band gap is still too large to explain the superconducting transition, observed experimentally at a few Kelvin. Nonetheless, other possible scenarios should be taken into account, such as the possibility that the tubes might be doped with electrons from the metal electrodes. Further, it has been recently shown[21] that the growth of defective tubes with portions of different chiralities along the same channel is possible, a scenario that would also affect the characterization of the superconducting transition. Accounting for the difficulty in modeling the growth mechanisms,[44] such semiempirical study provides a valuable insight into the possible structure of AFI-inserted small diameter nanotubes. One notes, however, that such conclusions concerning the topology of 4 Å tubes may not apply to the case of superconducting multiwall tubes inserted in larger zeolites.[16]

ACKNOWLEDGMENTS

We acknowledge interesting discussions with J. V. Alvarez, D. Carpentier, and G.-M. Rignanese. Calculations have been performed at the French CNRS national computing center (IDRIS, Orsay) and New York Center for Computational Sciences (NYCCS). This project is partly funded through the ANR-06-NANO-069-02 "Accent" contract. M.V.F.-S. acknowledges funding from a Marie-Curie Ext project under Contract No. MEXT-CT-2005-023311.

[1] M. Kociak, A. Y. Kasumov, S. Gueron, B. Reulet, I. I. Khodos, Y. B. Gorbatov, V. T. Volkov, L Vaccarini, and H. Bouchiat, Phys. Rev. Lett. **86**, 2416 (2001).

[2] A. Yu. Kasumov, M. Kociak, M. Ferrier, Yu. A. Kasumov, S. Gueron, B. Reulet, I. I. Khodos, Yu. B. Gorbatov, V. T. Volkov, L. Vaccarini, and H. Bouchiat, Physica B **329-333**, 1321 (2003).

[3] Z. K. Tang, L. Zhang, N. Wang, X. X. Zhang, G. H. Wen, G. D. Li, J. N. Wang, C. T. Chan, and P. Sheng, Science **292**, 2462 (2001).

[4] J. González, Eur. Phys. J. B **36**, 317 (2003).

[5] J. González and J. V. Alvarez, Phys. Rev. B **70**, 045410 (2004).

[6] J. González and E. Perfetto, Phys. Rev. B **72**, 205406 (2005).

[7] David Carpentier and Edmond Orignac, Phys. Rev. B **74**, 085409 (2006).
[8] Kenji Kamide, Takashi Kimura, Munehiro Nishida, and Susumu Kurihara, Phys. Rev. B **68**, 024506 (2003).
[9] D. Connétable, G.-M. Rignanese, J.-C. Charlier, and X. Blase, Phys. Rev. Lett. **94**, 015503 (2005).
[10] K.-P. Bohnen, R. Heid, H. J. Liu, and C. T. Chan, Phys. Rev. Lett. **93**, 245501 (2004).
[11] K. Iyakutti, A. Bodapati, X. Peng, P. Keblinsi, and S. K. Nayak, Phys. Rev. B **73**, 035413 (2006).
[12] Ryan Barnett, Eugene Demler, and Efthimios Kaxiras, Phys. Rev. B **71**, 035429 (2005).
[13] J.-C. Charlier, X. Blase, and S. Roche, Rev. Mod. Phys. **79**, 677 (2007).
[14] Lorin X. Benedict, Vincent H. Crespi, Steven G. Louie, and Marvin L. Cohen, Phys. Rev. B **52**, 14935 (1995).
[15] O. Dubay, G. Kresse, and H. Kuzmany, Phys. Rev. Lett. **88**, 235506 (2002).
[16] I. Takesue, J. Haruyama, N. Kobayashi, S. Chiashi, S. Maruyama, T. Sugai, and H. Shinohara, Phys. Rev. Lett. **96**, 057001 (2006).
[17] It is only when the inner tubes of the multiwall are connected to the leads that the SC transition can be observed.
[18] S. Piscanec, M. Lazzeri, J. Robertson, A. C. Ferrari, and F. Mauri, Phys. Rev. B **75**, 035427 (2007).
[19] Another reason to discard the study of C(3,3) tubes was shown by Connétable *et al.* (Ref. 9), by pointing out that the electronic density of states at the Fermi level in C(3,3) undistorted tubes is much smaller than that of C(5,0) tubes, therefore making C(3,3) tubes much less likely to be responsible of a superconducting T_c of several Kelvin.
[20] X. P. Yang, H. M. Weng, and J. Dong, Eur. Phys. J. B **32**, 345 (2003).
[21] T. Roussel, R. J.-M. Pellenq, and C. Bichara, Phys. Rev. B **76**, 235418 (2007).
[22] http://www.pwscf.org/
[23] J. M. Soler, E. Artacho, J. D. Gale, A. García, J. Junquera, P. Ordejón, D. Sánchez-Portal, J. Phys.: Condens. Matter **14**, 2745 (2002).
[24] N. Troullier and J. L. Martins, Phys. Rev. B **43**, 1993 (1991).
[25] David Vanderbilt, Phys. Rev. B **41**, 7892 (1990).
[26] D. M. Ceperley and B. J. Alder, Phys. Rev. Lett. **45**, 566 (1980).
[27] J. P. Perdew and A. Zunger, Phys. Rev. B **23**, 5048 (1981).
[28] J. P. Perdew, K. Burke, and M. Ernzerhof, Phys. Rev. Lett. **77**, 3865 (1996).
[29] N. David Mermin, Phys. Rev. **137**, A1441 (1965).
[30] E. Anglada, J. M. Soler, J. Junquera, and E. Artacho, Phys. Rev. B **66**, 205101 (2002).
[31] J. Junquera, O. Paz, D. Sánchez-Portal, and E. Artacho, Phys. Rev. B **64**, 235111 (2001).
[32] X. Blase, Lorin X. Benedict, Eric L. Shirley, and Steven G. Louie, Phys. Rev. Lett. **72**, 1878 (1994).
[33] S. Reich, C. Thomsen, and P. Ordejón, Phys. Rev. B **65**, 155411 (2002).
[34] While it is closer to the C_{2h} group, lowering the tolerance in the search for symmetry operations allows us to recover the original D_{5d} group; therefore, the final state is a superposition of both groups with a stronger C_{2h} character.
[35] Z. M. Li, Z. K. Tang, H. J. Liu, N. Wang, C. T. Chan, R. Saito, S. Okada, G. D. Li, J. S. Chen, N. Nagasawa, and S. Tsuda, Phys. Rev. Lett. **87**, 127401 (2001).
[36] Z. M. Li, Z. K. Tang, G. G. Siu, and I. Bozovic, Appl. Phys. Lett. **84**, 4101 (2004).
[37] M. Machón, S. Reich, C. Thomsen, D. Sanchez-Portal, and P. Ordejon, Phys. Rev. B **66**, 155410 (2002).
[38] P. Launois, R. Moret, D. Le Bolloc'h, P. A. Albouy, Z. K. Tang, G. Li, and J. Chen, Solid State Commun. **116**, 99 (2000).
[39] These authors have suggested that C(5,0) tubes, and not other 4 Å radius CNTs, grow preferentially inside the zeolite given the near match between the period of the tube with half of the period of the AFI crystal along the *c* axis. Indeed, this period coincides with the period of the oxygen rings forming the channels, which could also favor an attractive interaction between the tube and the matrix.
[40] This error is due to the finite size of the NAOs basis set and we correct it by means of the counterpoise approach.
[41] M. V. Fernández-Serra, Emilio Artacho, and José M. Soler, Phys. Rev. B **67**, 100101(R) (2003).
[42] V. Ermoshin, K. smirnov, and D. Bougeard, J. Mol. Struct. **410**, 371 (1997).
[43] B. W. H. van Beest, G. J. Kramer, and R. A. van Santen, Phys. Rev. Lett. **64**, 1955 (1990).
[44] J.-C. Charlier, X. Blase, A. De Vita, and R. Car, Appl. Phys. A: Mater. Sci. Process. **68**, 267 (1999).